

# Spectroscopic investigation and density functional theory calculations of mercaptobenzothiazole and mercaptobenzimidazole ligands and their rhenium complexes

Noura AlHokbany<sup>1\*</sup>, Ibrahim AlJammaz<sup>2</sup>

<sup>1</sup>\*Department of chemistry, College of Science, King Saud University, Riyadh, Kingdom of Saudi Arabia;

<sup>2</sup>Cyclotron and Radiopharmaceuticals Department, King Faisal Specialist Hospital and Research Center, Riyadh, Kingdom of Saudi Arabia

Email: [nhokbany@ksu.edu.sa](mailto:nhokbany@ksu.edu.sa)

Received 22 April 2011; revised 1 July 2011; accepted 11 July 2011.

## ABSTRACT

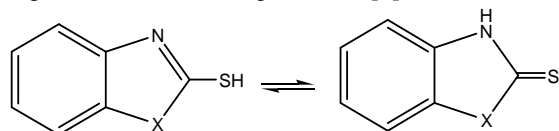
Four complexes containing the  $[\text{Re}(\text{V})\text{O}]^{3+}$  core have been prepared by substitution on the precursors  $\text{ReO}(\text{citrate})_2^-$  and  $\text{ReO}(\text{gluconate})_2^-$ . The complex  $[\text{ReO}(\text{MBT})_2\text{OH}]$  was obtained by reaction of the direct reduction of  $\text{ReO}_4^-$  using sodium borohydride as a reducing agent. Four complexes were characterized by UV-Vis and IR spectrophotometer, elemental analyses,  $^1\text{H}$ - and  $^{13}\text{C}$  NMR spectroscopy, TG and DFT calculations.

**Keywords:**  $[\text{ReO}]^{3+}$ , DFT, Mercaptobenzothiazole Ligand, Mercaptobenzimidazol Ligand, TG/DTA, XPS, Rhenium Complexes.

## 1. INTRODUCTION

Heterocyclic thiolates are electron-rich and multifunctional ligands, that show various coordination modes and form monomeric or polymeric complexes [1]. They can act as unidentate or bidentate ligands in metal complexes.

Mercapto-1,3-azole ligands play an important role in industry and medicine [2]. One of their attractive features is their acidity, which could influence their chemical reactivity toward transition metal ions and determine the structure of the final complexes. These small molecules exist as two tautomeric conformations exhibiting thiol-thione isomerism involving  $-\text{NH}-\text{C}=\text{S}$  and  $-\text{N}=\text{C}-\text{SH}$  groups in a thione-thiol equilibrium [3].



X= NH, O, S

Probably, only two atoms can act as bonding sites; the sulfur exocyclic atom and the cyclic nitrogen atom. Because the lone pairs on the oxygen or sulfur atoms are involved in the resonating structures of the molecules, we may expect that they should have no coordinating abilities. To investigate this and as part of our research into rhenium (Re) chemistry, we decided to investigate the chemical behavior of ambidentate ligands such as 2-mercaptoben-zothiazole (MBT) and 2-mercaptobenzimidazole (Bimz).

The coordination chemistry of Re has been explored because of its use in radiopharmaceuticals. Rhenium radiopharmaceuticals are a class of therapeutic agents in which the biodistribution is determined by the size, charge and lipophilicity of the complex. Among these compounds, the chemistry of oxo rhenium complexes is of particular interest. The interesting chemistry results from the favorable nuclear properties of  $^{186}\text{Re}$  and  $^{188}\text{Re}$  nuclides, which make the radioisotopes useful for diagnostic nuclear medicine and applications in radioimmunotherapy [4]. Our aim was to study the chemical properties of mercaptobenzothiazole ligands toward the  $[\text{Re}=\text{O}]^{3+}$  core. In this paper, we describe the synthesis of oxorhenium complexes and the characterization of those complexes with several spectroscopic methods. In addition, density functional theory (DFT) calculations of some representative compounds are also discussed.

## 2. EXPERIMENTAL

### 2.1. Materials and Methods

All the reagents used to the synthesis were commercially available and were used without further purification.  $\text{ReO}(\text{citrate})_2^-$  and  $\text{ReO}(\text{gluconate})_2^-$  precursors were prepared according to literature [5,6] respectively. IR spectroscopy was recorded on a Perkin Elmer spectro-

photometer 1000 in the spectral range 200 - 4000  $\text{cm}^{-1}$  with sample in the form of KBr pellets. UV-Vis spectra were recorded on UV-Vis Beckman Du-70 spectrophotometer in the range 190 - 700 nm.  $^1\text{H}$ - $^{13}\text{C}$  NMR spectra were measured in ( $\text{DMSO-d}_6$  and  $\text{CDCl}_3$ ) as solvents on a JOEL-NMR 400 MHz spectrometer. Micro-analytical (CHN) were run at the Mikronalytisches Labor Pascher, Germany. Thermogravimetric/differential Thermal analysis (TG/DTA) measurements were carried out using Perkin- Elmer TG A7 thermal analyzer, the weight loss was measured from ambient temperature up to 1000°C at a heating rate of 10°C/min. About 15 mg of the compound was used for the analysis, with alumina as the reference material. Mass spectroscopy was run on Quattra Gas chromatography mass spectrometer run at the Mikronalytisches Labor Pascher, Germany.

## 2.2. Synthesis of Complexes

### 2.2.1. $[\text{ReO}_2(\text{MBT})(\text{H}_2\text{O})_2] \text{I}$

$\text{NaReO}_4$  (1 mmol, 0.273 g) was added to a solution of  $\text{SnCl}_2$  (1 mmol, 0.256 g) in citric acid (0.5 M, 5 mL). MBT (3 mmol, 0.501 g) in ethanol was added dropwise to the mixture. The mixture was stirred at room temperature for 3hr. The pH was adjusted to 9 with NaOH (0.5M) [6]. The blackgreen precipitate was filtrated and washed with ethanol and acetone to obtain green crystals, (89% yield) of compound: UV-Vis ( $\text{CH}_2\text{Cl}_2$ );  $\lambda_{\text{max}}[\text{nm}](\epsilon; \text{dm}^3 \text{mol}^{-1} \text{cm}^{-1})$ : 205(1582), 219(1044), 355 (1499).  $^1\text{H}$  NMR ( $\text{d}_6\text{-DMSO}$ , ppm): 7.7(m,Ha,Hc), 7.4(m,Hb), 7.2(m,Hd) ring.  $^{13}\text{C}$  NMR ( $\text{CDCl}_3$ , ppm): 122, 123, 126, 127(C=C), 133(C=C-S), 189(S=C), 141(C=C-C-N). IR (KBr,  $\nu/\text{cm}^{-1}$ ): 914, 860 (O=Re=O), 624 (Re-N), 569 (Re-S). MS (m/z): 420[M]<sup>+</sup>. Anal. Calc. (Found) for  $\text{C}_7\text{H}_8\text{S}_2\text{NO}_4\text{Re}$ : C, 20. (19.97); H, 1.9 (1.78); N, 3.33 (3.01); Re, 44.3(42.2)%.

### 2.2.2. $[\text{ReO}_2(\text{Bimz})(\text{H}_2\text{O})_2] \text{II}$

$\text{NaReO}_4$  (1 mmol, 0.273 g) was added to a solution of  $\text{SnCl}_2$  (1 mmol, 0.2256 g) in citric acid (0.5 M, 5mL). Followed by the dropwise addition of Bimz (3mmol, 0.45gm) in EtOH. The mixture was stirred at room temperature for 3hr. The pH was adjusted to 9 with NaOH (0.5 M). Filtration the blackgreen precipitate and washed with ethanol and acetone to obtain the yellow powder , 89.7% yield of compound: UV-vis ( $\text{CH}_2\text{Cl}_2$ ;  $\lambda_{\text{max}}[\text{nm}](\epsilon; \text{dm}^3 \text{mol}^{-1} \text{cm}^{-1})$ : 190(1911), 245(456).  $^1\text{H}$  NMR ( $\text{d}_6\text{-DMSO}$ , ppm): 12.2(s,NH), 7.7(m,Ha,Hc), 7.4(m,Hb), 7.2(m,Hd) ring.  $^{13}\text{C}$  NMR ( $\text{CDCl}_3$ , ppm): 122,123,126, 127(C=C), 133(C=C-C-S), 189(S=C), 141(C=C-C-N). IR (KBr,  $\nu/\text{cm}^{-1}$ ): 909, 843 (O=Re=O), 618 (Re-N), 547 (Re-S). MS (m/z): 402[M]<sup>+</sup>. Anal. Calc. (found) for  $\text{C}_7\text{H}_8\text{SN}_2\text{O}_4\text{Re}$ : C, 20.8(19.89); H, 1.99 (1.57); N, 6.9 (6.24); Re, 46.3 (44.7) %.

### 2.2.3. $[\text{ReO}(\text{Bimz})_2\text{OH}] \text{III}$

Rhenium (V)(gluconate)<sub>2</sub><sup>-</sup> (14.8 mL ,1 mmol) solution was adjusted to pH 10 by NaOH (0.1 M) followed by addition of Bimz (3 mmol, 0.450 g) dissolved in 1mL of methanol. After stirring for 1hr, to the mixture was addition of methanol to precipitate. 89% yield of compound: UV-vis ( $\text{H}_2\text{O}$ ;  $\lambda_{\text{max}}[\text{nm}](\epsilon; \text{dm}^3 \text{mol}^{-1} \text{cm}^{-1})$ : 240(3000), 325(2060).  $^1\text{H}$  NMR ( $\text{d}_6\text{-DMSO}$ , ppm) 7.1(m, Hb), 7.1(m, Hc), 7.3 (m,Hd), 7.6(m,Ha):  $^{13}\text{C}$  NMR ( $\text{DMSO}$ , ppm): 112(C=C), 121(C=C-N), 179(C=N). IR (KBr,  $\nu/\text{cm}^{-1}$ ): 908 (Re=O), 619(Re-N), 415(Re-O). Anal. Calc.(found) for  $\text{C}_{14}\text{H}_9\text{N}_4\text{O}_2\text{S}_2\text{Re}$ : C,32.6(31.9); H, 1.74(1.85); N, 10.86(9.76)%.

### 2.2.4. $[\text{ReO}(\text{MBT})_2\text{OH}] \text{IV}$

To a solution of  $\text{NaReO}_4$  (1 mmol, 0.2731 g), MBT (3 mmol, 0.501g) in methanol was dropwise added. The reducing agent  $\text{NaBH}_4$  (1 mmole) in (0.1 KOH pH 8) was added and the color of solution changed to bronze. The mixture was stirred at reflux for 3 hr, followed by evaporation to almost dryness, the gray precipitate recrystallized by hot methanol [5]. 86 % yield of compound: UV-vis ( $\text{CH}_2\text{Cl}_2$ ;  $\lambda_{\text{max}}[\text{nm}](\epsilon; \text{dm}^3 \text{mol}^{-1} \text{cm}^{-1})$ : 205(1582), sh 219( 1044), 355(1499).  $^1\text{H}$  NMR ( $\text{d}_6\text{-DMSO}$ , ppm): 7.7(m, Ha, Hc), 7.4(m, Hb), 7.2(m, Hd) ring, 1.2(s,OH).  $^{13}\text{C}$  NMR ( $\text{DMSO}$ , ppm): 122,123, 126,127(C=C), 190(S=C), 141(C=C-C-N). IR (KBr,  $\nu/\text{cm}^{-1}$ ): 912 (Re=O), 661 (Re-N), 649 (Re-S), 432 (Re-O). MS (m/z): 570[M]<sup>+</sup>. Anal. Calc. (found) for  $\text{C}_{14}\text{H}_{12}\text{S}_4\text{N}_2\text{O}_2\text{Re}$ : C, 29.3(29.12); H, 2.09(2.28); N, 4.91(5.12); Re, 32.6(30.9)%.

## 3. RESULTS AND DISCUSSION

### 3.1. Computational Details

The GAUSSIAN 03 program [7] was used in the calculations. The complexes were treated as open shell-system and no symmetry constraints were applied. Geometrical optimization of the investigated complex was carried out with Beck's three parameter exchange functional B3LYP using the Los Alamos LANL2DZ spilt-valence basis set [8,9]. A harmonic vibrational analysis was performed following the geometrical optimization of the complex at the same level of theory B3LYP and the same basis set [10]. An additional d function with exponent a = 0.3811 and an f function with exponent a = 2.033 on the rhenium atom were added. Natural bond orbital (NBO) calculations were performed with the NBO code [11] included in GAUSSIAN 03. The optimized geometry for various forms of the MBT molecule is shown in **Figure 1**. The two tautomeric forms of MBT were subjected to geometry optimization at B3LYP/6-31G\*\* (**Table 1**).

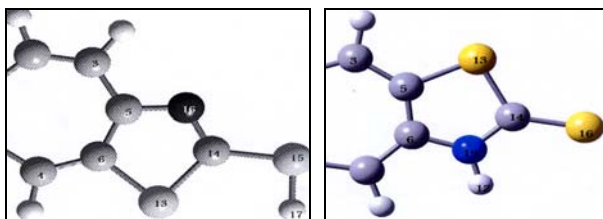


**Figure 1.** Optimized geometry of MBT monomer in thiol(a) and thione (b) tautomeric equilibrium at B3LYP/6-31G\*\*

**Table 1.** Selected optimized bond lengths (Å) and angles(°) for MBT and Bimz ligands.

Bond length (Å)	Bond angles (°)	B3LYP/LANL2DZ
<b>MBT</b>		
S(15)-C(14) 1.8159	-S(15)-C(14)H(17)	96.102
S(15)-H(17) 1.3784	S(13)-C(14)-N(16)	113.8972
C(14)-N(16) 1.2948	S(13)-C(5)-C(6)	109.04
N(16)-C(6) 1.3918	C(14)-N(16)-C(6)	114.22
C(14)-S(13) 1.8411	C(4)-C(6)-N(16)	117.562
<b>Bimz</b>		
C(8)-S(15) 1.812	N(7)-C(8)-N(9)	113.3
C(8)-N(9) 1.393	C(8)-S(15)-H(16)	94.2
N(9)-H(14) 1.010	C(8)-N(9)-H(14)	126.2
N(7)-C(8) 1.325	N(9)-C(8)-S(15)	120.7
S(15)-H(16) 1.373	C(2)-N(9)-H(14)	106.8

### 3.2. *cis*-dioxo [ReO<sub>2</sub>(MBT)(H<sub>2</sub>O)<sub>2</sub>]

The most important bond lengths and angles for the compound are reported in **Table 2**. The transformation from the ideal octahedral to the distorted octahedral seen in complexes is mainly attributed to the electronic repulsion of the short Re=O bond. For the [ReO<sub>2</sub>(MBT)(H<sub>2</sub>O)<sub>2</sub>] complex, the bridging N-S ligands introduce some additional strain (**Figure 2**).

The Re-N, Re=O<sub>terminal</sub> and Re-O bonds lengths in the

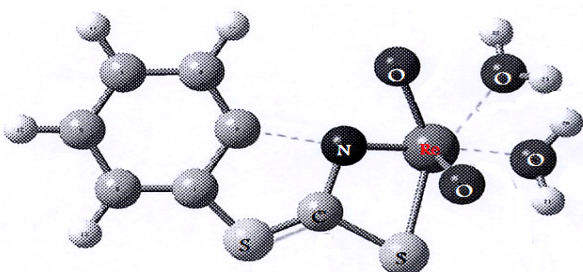


**Figure 2.** Optimized structure of [ReO<sub>2</sub>(MBT)(H<sub>2</sub>O)<sub>2</sub>].

**Table 2.** Selected optimized bond lengths (Å) and angles(°) for [ReO<sub>2</sub>(MBT)(H<sub>2</sub>O)<sub>2</sub>]

Bond length (Å)	Bond angles (°)	B3LYP/LANL2DZ
Re(15)-O(16) 2.0733	O(16)-Re(15)-O(17)	159.9
Re(15)-O(17) 1.6954	O(17)-Re(15)-N(9)	100.288
Re(15)-N(9) 2.1597	S(14)-Re(15)-N(9)	53.262
Re(15)-S(14) 3.3475	S(14)-Re(15)-O(18)	132.96
Re(15)-O(19) 2.094	N(9)-Re(15)-O(19)	156.40
Re(15)-O(18) 3.6705	N(9)-C(8)-S(14)	121.33

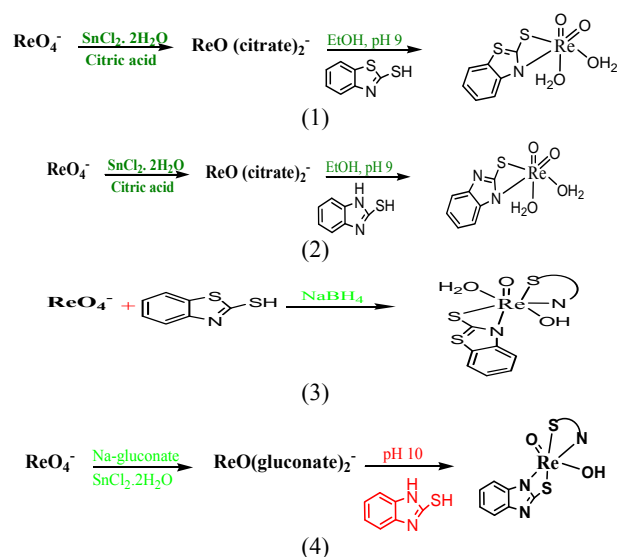
[ReO<sub>2</sub>(MBT)(H<sub>2</sub>O)<sub>2</sub>] complex agree with comparable values found in rhenium compounds with a Re=O core [13,14]. The mean Re=O<sub>terminal</sub> bond lengths of 1.680 and 1.712 Å correspond to the values reported for mononuclear mono-oxo d<sup>2</sup> rhenium complexes with an average bond length of 1.70 Å [15]. These results suggest that a small amount of overlap also occurs between the *d<sub>xz</sub>* and *d<sub>yz</sub>* rhenium orbitals and the suitable p orbitals of the O ligands. An ideal single Re-O bond length, predicated by the use of Pauling's oxygen covalent radius and Cotton and Lippard's value for the Re (V) octahedral covalent radius, should be around 2.04 Å [16]. **Tables 3** and **4** present the atomic charge determined from the natural population analysis (NPA) for the complexes. The calculated charge on the rhenium atom is considerably lower than the formal charge of +5 (1.343).

### 3.3. [ReO(MBT)2OH]

The most important bond lengths and angles for the compound are reported in **Table 5**. The gas phase structural optimization shown in **Figure 3** indicates that the complex has a tetrahedral geometry. However, in the presence of a solvent, the attachment of solvent molecules to form distorted square pyramidal structures has been confirmed by measuring the absorption spectra of the complexes in different solvent and recording the change in wave length caused by a variety of solvents.

### 3.4. The Analytical Data

**Table 6** summarizes some analytical data and properties of the prepared complexes. The reaction gives oxorhenium complexes in good yields. The elemental analysis provides a good agreement between the experimental data and the calculated values (**Scheme 1**).



**Scheme 1.** Synthesis of complex.

### 3.5. The IR spectra

In the IR spectrum, a weak broad band was observed with a maximum at  $3445\text{ cm}^{-1}$ , shown in **Figure 4**. This band was predicted at  $3526\text{ cm}^{-1}$  in the DFT calculation of monomeric MBT thione (II) for NH stretching vibrations, as shown in **Table 7**. This result indicates the existence of a monomeric thione form of MBT. Our *ab initio* calculations for MBT explain the bands at  $3115$  and  $3069\text{ cm}^{-1}$  as symmetric and asymmetric NH stretching vibrations, and the peak observed at  $3041\text{ cm}^{-1}$  can be explained as asymmetric CH stretching vibrations (**Figure 5**).

Our calculations predicted that the intense bands observed at  $1244$ ,  $1425$  and  $1495\text{ cm}^{-1}$  are associated to the vibrations of C-N-H group. The intense band observed at  $1455\text{ cm}^{-1}$  is a result of attributed to CC and CN stretch-

**Table 3.** Atomic charges from the Natural Population analysis (NPA) for  $[\text{ReO}_2(\text{MBT})(\text{H}_2\text{O})_2]$

Atom	Atomic charge
Re(15)	1.3439
O(16)	-1.0824
N(9)	-0.56149
O(17)	-0.73924
S(14)	0.61039
O(18)	0.0332
O(19)	0.0854

**Table 4.** The occupancies and hybridization of the calculated natural bond orbitals (NBOs) of  $[\text{ReO}_2(\text{MBT})(\text{H}_2\text{O})_2]$ .

BD(2-center bond)	occupancy	Hybridization of NBO
Re(15)-O(17)	1.87533(0.3761)	$0.6133(\text{sd})_{\text{Re}} + 0.7899(\text{p})_{\text{O}}$
Re(15)-N(9)	1.7159(0.8298)	$0.9109(\text{sp})_{\text{N}} + 0.412(\text{sd})_{\text{Re}}$
O(18)-H(20)	1.9582(0.7713)	$0.8782(\text{sp})_{\text{O}} + 0.478(\text{s})_{\text{H}}$

**Table 5.** Selected optimized bond lengths ( $\text{Å}$ ) and angles ( $^\circ$ ) for  $[\text{ReO}(\text{MBT})_2\text{OH}]$

Bond length ( $\text{Å}$ )	Bond angles ( $^\circ$ )	B3LYP/LANL2DZ
Re(29)-O(31) 1.696	O(31)-Re(29)-S(27)	113.971
Re(29)-O(30) 1.881	O(30)-Re(29)-S(28)	100.2773
Re(29)-S(27) 2.355	Re(29)-O(30)-H(32)	131.865
Re(29)-S(28) 2.336	S(27)-Re(29)-S(30)	110.951

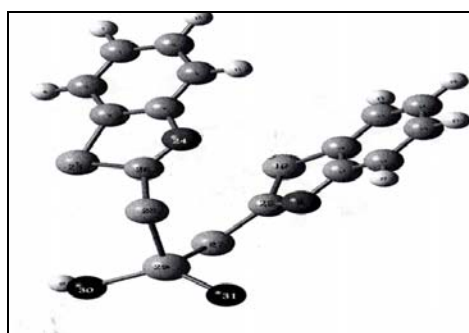


**Figure 3.** Optimized structure of  $[\text{ReO}(\text{MBT})_2\text{OH}]$ .

**Table 6.** The analytical data of complexes.

Complex/ Theoretical Formula	Color	Yield %	Decomposition Temp $^\circ\text{C}$	Elemental Analysis % Calc.(Found)			
				C	H	N	Re
$[\text{ReO}_2(\text{MBT})(\text{H}_2\text{O})_2]$ I $\text{C}_7\text{H}_8\text{S}_2\text{NO}_4\text{Re}$	Dark-green	89	300	20.0 (20.02)	1.9 (1.78)	3.33 (3.20)	44.3 (42.2)
$[\text{ReO}_2(\text{BImz})(\text{H}_2\text{O})_2]$ II $\text{C}_7\text{H}_8\text{SN}_2\text{O}_4\text{Re}$	Yellow	89.7	300	20.8 (20.52)	1.99 (1.95)	6.90 (6.24)	46.30 (44.7)
$[\text{ReO}(\text{Bimz})_2\text{OH}]$ III $\text{C}_{14}\text{H}_9\text{N}_4\text{O}_2\text{S}_2\text{Re}$	Gray	98	300	32.60 (32.33)	1.74 (1.85)	10.86 (10.78)	
$[\text{ReO}(\text{MBT})_2\text{OH}]$ IV $\text{C}_{14}\text{H}_{12}\text{S}_4\text{N}_2\text{O}_2\text{Re}$	Green	86	300	29.3 (29.12)	2.09 (2.28)	4.91 (4.82)	32.6 (30.99)

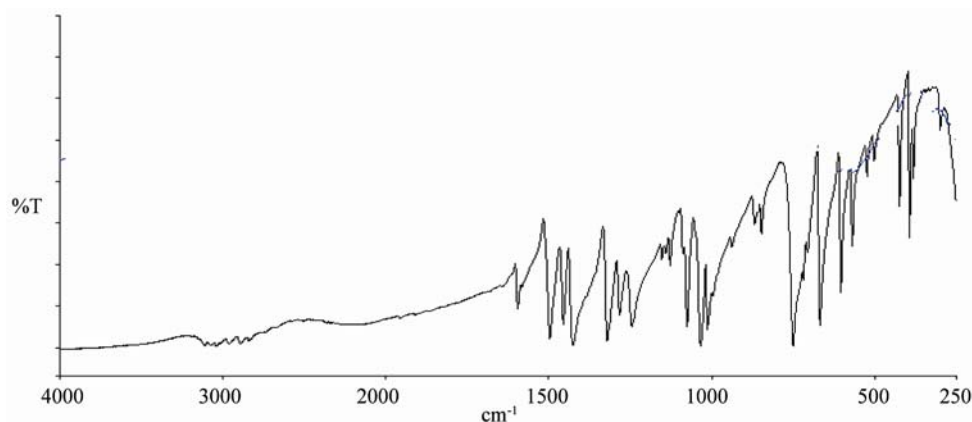


**Figure 4.** IR spectra of (MBT) ligands .

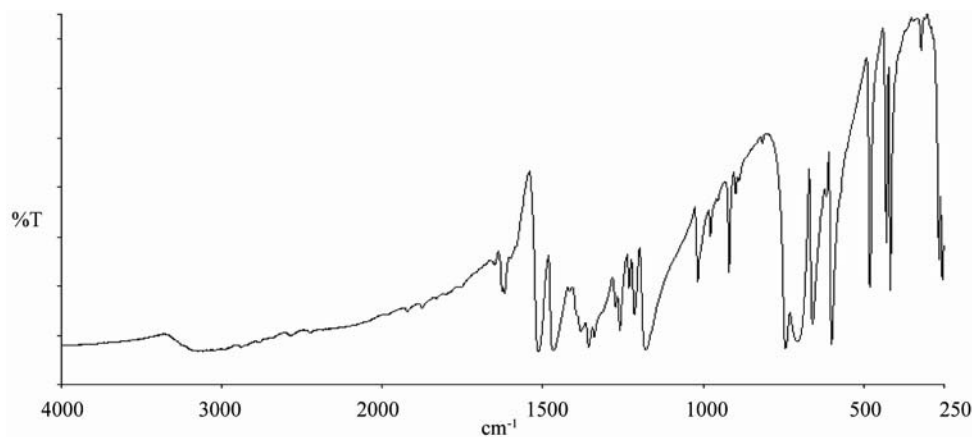


**Figure 5.** IR spectra of (Bimz) ligands

ing and CH bending vibrations. The strong bands at 1012, 1033 and 1076  $\text{cm}^{-1}$  are predicted to N-C = S group in addition to CCC and CH bending vibrations [18, 19]. The very weak bands observed at 2640 and 2480  $\text{cm}^{-1}$  can be interpreted as overtone bands of the fundamental frequencies at 1319 and 1244  $\text{cm}^{-1}$ . The band observed at  $-1595 \text{ cm}^{-1}$  is ascribed to a C=C stretching mode. The intense band observed at 1455  $\text{cm}^{-1}$  is attributed to CC, CN stretching and CH bending vibrations. The strong bands at 1012, 1033 and 1076  $\text{cm}^{-1}$  represent the N-C=S group in addition to CCC and CH bending vibrations. The symmetric out-of-plane CH vibration was observed as a very strong band at 750  $\text{cm}^{-1}$ . The strong band observed at 668  $\text{cm}^{-1}$  and the weak bands at 603 and 706  $\text{cm}^{-1}$  were attributed to C-S stretching modes [19]. It should be mentioned that the theoretical values are usually higher than the experimental data. It is necessary to scale the theoretical data by an optimal scaling factor (0.996) that varies with the basis set [20].

From **Figure 6 (C)** IR spectra of complex  $[\text{ReO}_2(\text{MBT})(\text{H}_2\text{O})_2]$  showed two characteristic peaks, at 914 and 860  $\text{cm}^{-1}$ , and  $[\text{ReO}_2(\text{Bimz})(\text{H}_2\text{O})_2]$  assigned at 908, 843  $\text{cm}^{-1}$ . These values are typical of *cis*-dioxo O=Re=O group of the *cis*-dioxorhenium(V) coordinated complexes [17,21]. In **Figure 6. (B)** show that  $\nu\text{Re}=\text{O}$  has been detected on 912  $\text{cm}^{-1}$  for complex  $[\text{ReO}(\text{MBT})_2\text{OH}]$ , and  $\nu\text{Re}-\text{O}$  and  $\nu\text{Re}-\text{S}$  at 649 and 432  $\text{cm}^{-1}$ , respectively as compare with free ligand (A) MBT. In **Figure 7 (C)** as shown that  $\nu\text{Re}=\text{O}$  has been detected on 908  $\text{cm}^{-1}$  and absences of the medium band for  $\nu\text{NH}$  at 3117  $\text{cm}^{-1}$  and the coordinated bonded at  $\nu\text{Re}-\text{N}$ ,  $\nu\text{Re}-\text{O}$  and  $\nu\text{Re}-\text{S}$  at 546, 415 and 619  $\text{cm}^{-1}$ , respectively. The infrared spectra of the rest complexes show bands in the region 3304 - 3458  $\text{cm}^{-1}$  corresponding to  $\nu$  OH stretching and the bands at 1650 - 1580  $\text{cm}^{-1}$  vibration due to HOH bending. Some bands are disappearing in some complexes such as SH and NH at  $-2889$  and  $-3117 \text{ cm}^{-1}$  respectively, these indicating that these donor atoms were de-

protonated upon complexation.

### 3.6. The NMR spectra

The  $^1\text{H}$  NMR spectra of a series of mercapto complexes show signals assigned to the Ha,b,c,d (the protons of the benzene ring) in different chemical shifts caused by the anisotropic effect, which laminated the protons oriented toward the oxygen that appear deshielded relative to the other protons oriented away from the oxygen ( toward or away from the oxo-metal core) [18] (**Figure 8**).

As we see the protons near the Re=O core was assigned to the downfield region of the spectrum at  $-7.7 - 7.6 \text{ ppm}$  [16-20]. The Bimz-complexes demonstrate the same chemical shift behavior as the MBT-complexes. The  $^{13}\text{C}$  NMR spectra of the complexes exhibit two new characteristic peaks for C=S and C-N at lower fields of 189 and 141 ppm compared with the spectra of free ligand MBT, indicating that coordination *via* the charged thiolic sulfur and nitrogen atoms occurred (**Figures 9-11**). All of the NMR spectra

**Table 7.** The vibrational assignment, experimental and calculated wave numbers in  $\text{cm}^{-1}$  of MBT and Bimz.

Experimental	B3LYP/LANL2DZ	Assignment
<b>MBT</b>		
3445	3526	NH
3115(vw)	3526	Asymmetric NH str.
3041, 2889	3187	Asymmetric CH str.
1595	1671	C=C str.
1497,1425,1244	1508	C-C str. , (C-N-H)
1012,1033,1076	1234, 1342	(N-C=S), C=S
750,668	963	Out.o.p. asym
706, 603	885	C-S
394	438	S-C=S bend.
<b>Bimz</b>		
3455	3684	NH
3117 (vw)	3210	Asymmetric NH str.
2880	2990	Asymmetric CH str.
1618	1671	C=C str.
1466, 1356	1506	C-C str. , (C-N-H)
1178	1199	(N-C=S), C=S
743,659	962	Out.o.p. asym
1513	1633	C=N



**Table 8.** The NMR data for ligand and complexes. ( $\delta$ , ppm)<sup>a</sup>

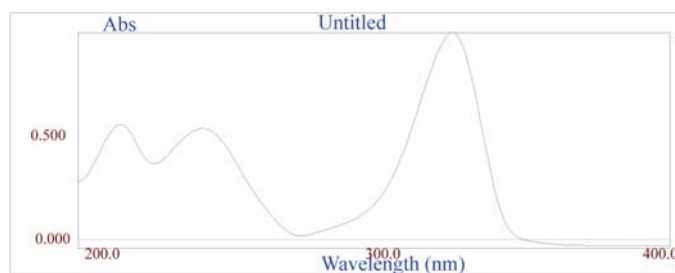
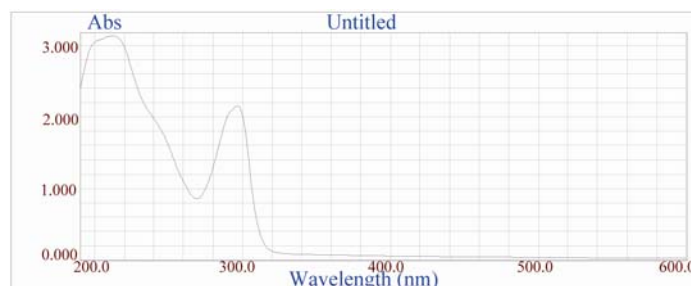
Compounds	<sup>1</sup> H NMR ( $\delta$ , ppm) ; Assignment	<sup>13</sup> C NMR ( $\delta$ , ppm) ; Assignment
MBT	3(s,SH), 8.1(d,1H), 7.55 (m, 2H), 8.23 (s,1H)	122,123,126,127 (C=C), 133(C=C-C-S), 153(C-N), 156 (N=C)
[ReO <sub>2</sub> (MBT) (H <sub>2</sub> O) <sub>2</sub> ] <b>I</b>	7.7(m,2H), 7.4(m,1H), 7.2(m,1H) ring	122, 123,126,127(C=C), 133(C=C-C-S), 189(S=C),141(C=C-C-N)
Bimz	3(s,SH), 5(s,NH),7.7(d,1H),7.26(m,2H), 7.7(s,1H) ring	122, 123,115,115(C=C), 137(C-C-N), 141(N=C-S)
[ReO <sub>2</sub> (Bimz) (H <sub>2</sub> O) <sub>2</sub> ] <b>II</b>	7.1(m, 2H),7.5(m, 1H ), 7.6(s,1H) ring	110(C=C), 122(C=C-N), 132(C-N), 168(C=N).
[ReO(Bimz) <sub>2</sub> OH] <b>III</b>	7.1(m, 1H), 7.1(m, 1H ), 7.3(m,1H), 7.6(m,1H)	112(C=C), 121(C=C-N), 179(C=N). 45(CH <sub>2</sub> )
[ReO(MBT) <sub>2</sub> OH] <b>IV</b>	7.7(m,2H), 7.4(m,H1), 7.2(m,1H) ring,	122, 124,127,129,113(C=C-S), 141(C=C-C-N), 190(S=C).

<sup>a</sup> s=singlet, d=doublet, t=triplet, m=multiplet**Table 9.** The Electronic data of free ligands and complexes.

Compound	$\lambda_{max}$ [nm] ( $\epsilon$ ; dm <sup>3</sup> mol <sup>-1</sup> cm <sup>-1</sup> )	Assignment
MBT	212 (519), 247 (767)	$\pi \rightarrow \pi^*$ , $n \rightarrow \pi^*$
[ReO <sub>2</sub> (MBT) (H <sub>2</sub> O) <sub>2</sub> ] <b>I</b>	205 (1582), 219 (1044), 355 (1499)	$\pi \rightarrow \pi^*$ , $\pi \rightarrow \pi^*$ , $\pi(O) \rightarrow d$
Bimz	224 (3080), 244 (3429), 298 (3161)	$\pi \rightarrow \pi^*$ , $\pi \rightarrow \pi^*$ , $n \rightarrow \pi^*$
[ReO <sub>2</sub> (Bimz) (H <sub>2</sub> O) <sub>2</sub> ] <b>II</b>	190(1911), 245 nm(456), 300(315)	$\pi \rightarrow \pi^*$ , $n \rightarrow \pi^*$ , $\pi(O) \rightarrow d$
[ReO(Bimz) <sub>2</sub> OH] <b>III</b>	240(3000), 325(2060)	$\pi \rightarrow \pi^*$ , $\pi(O) \rightarrow d$
[ReO(MBT) <sub>2</sub> OH] <b>IV</b>	209( 1556), 233 ( 1055 ), 359 (1498)	$\pi \rightarrow \pi^*$ , $\pi \rightarrow \pi^*$ , $\pi(O) \rightarrow d$

**Table 10.** Mass spectra data of Re-complexes.

Complexes	$\approx$ Mwt	Most relative intensity (m/z)
[ReO <sub>2</sub> (MBT) (H <sub>2</sub> O) <sub>2</sub> ] <b>I</b>	420	ReO <sub>2</sub> (218), ReO <sub>2</sub> (MBT)(385), MBT(167), Benzothazole (135),Bz(95,78, 61,44).
[ReO <sub>2</sub> (Bimz) (H <sub>2</sub> O) <sub>2</sub> ] <b>II</b>	402	ReO <sub>2</sub> (Bimz)(355), Re(Bimz)(336),Bimz(148), Bz(95,78, 61,44).
[ReO(MBT) <sub>2</sub> OH] <b>IV</b>	570	ReO(MBT) <sub>2</sub> (553), 2MBT (268), MBT(167), Methyl-MBT(181), Benzothazole(135),Bz(95,78, 61,44).

**Figure 12.** UV spectra of [ReO(MBT)<sub>2</sub>OH] complex.**Figure 13.** UV spectra of [ReO(Bimz)<sub>2</sub>OH] complex.

### 3.9. Thermal analysis of complexes

As noted in **Table 11** there is a good agreement between the calculated percentages of decomposition steps based on the proposed structures and the experimentally deter-

mined data. These results provide further evidence for the plausibility investigated structures. The black residue can be attributed to metal oxides (Re<sub>2</sub>O<sub>3</sub>, 27.4%) (**Figure 16**).

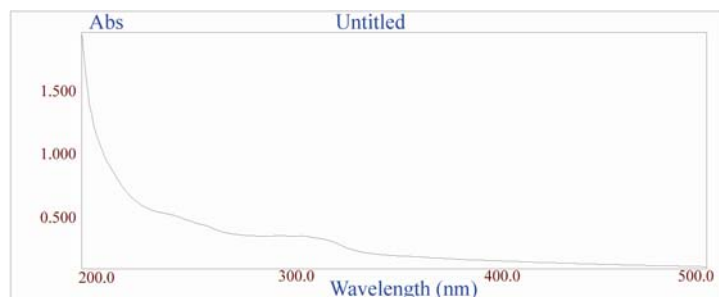


**Figure 14.** UV spectra of  $[\text{ReO}_2(\text{Bimz})(\text{H}_2\text{O})_2]$  complex.

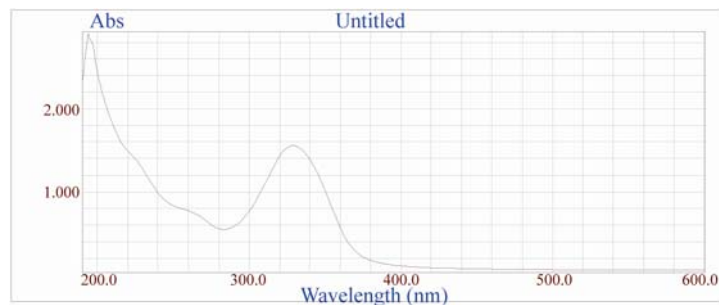
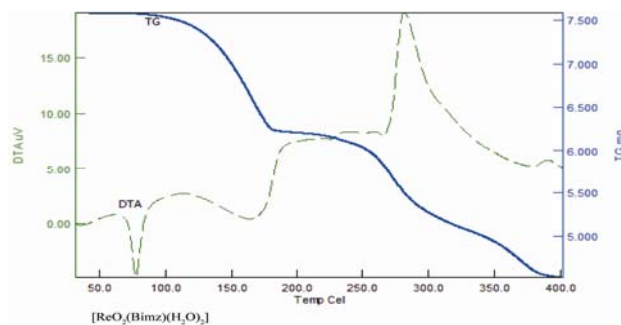


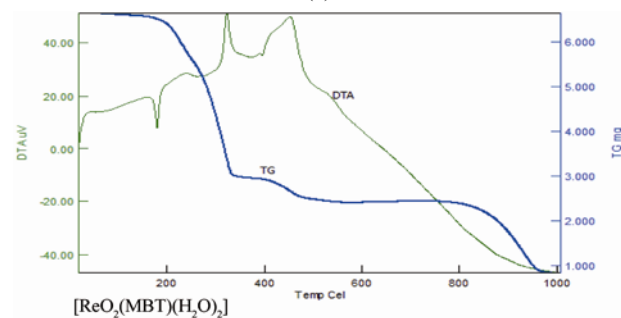
**Figure 15.** UV spectra of  $[\text{ReO}_2(\text{MBT})(\text{H}_2\text{O})_2]$  complex.

**Table 11.** The TG data of complexes.

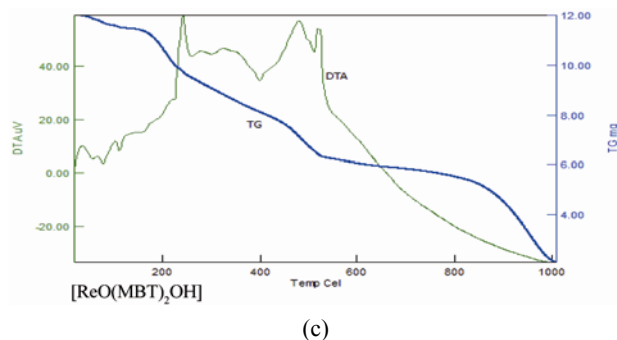
Complex	Decomposition step	Anal(Calc) %	Temp °C	Assignment
$[\text{ReO}_2(\text{MBT})(\text{H}_2\text{O})_2]$ I	First step	7.5 (8.5)	50 - 150	Loss of $2\text{H}_2\text{O}$
	Second step	37 (39.5)	200 - 600	Loss of MBT
$[\text{ReO}_2(\text{Bimz})(\text{H}_2\text{O})_2]$ II	First. step	7.6(8.9)	100 - 250	Loss of $2\text{H}_2\text{O}$
	Second. step	25.8(29)	250 - 600	Loss of Bimz
$[\text{ReO}(\text{MBT})_2\text{OH}]$ IV	First. step	4.99(6.11)	50 - 190	Loss of OH
	Second. step	58 (54)	200 - 600	Loss of 2MBT



(a)



(b)



(c)  
**Figure 16.** TG and DTA of complexes.

#### 4. CONCLUSIONS

The experiments showed that suitable complexation of monodentate and bi-dentate S/N and mono-dentate S/N ligands was able to stabilize the  $[\text{Re}^{\text{V}}=\text{O}]$  core. In this paper, we reported the synthesis of a series of novel oxorhenium (V) complexes,  $[\text{ReO}_2(\text{MBT})(\text{H}_2\text{O})_2]$  **I**,  $[\text{ReO}_2(\text{Bimz})(\text{H}_2\text{O})_2]$  **II**,  $[\text{ReO}(\text{Bimz})_2\text{OH}]$  **III**, and  $[\text{ReO}(\text{MBT})_2\text{OH}]$  **IV**. The compounds were fully characterized by means of spectroscopy methods. Density functional calculations for the  $[\text{ReO}_2(\text{MBT})(\text{H}_2\text{O})_2]$  **I** and  $[\text{ReO}(\text{MBT})_2\text{OH}]$  **IV** complexes were carried out using the DFT method with the B3LYP functional and LANL2DZ basis set. The experimentally characterized molecular structures of these complexes have been properly reproduced by the B3LYP method.

#### 5. ACKNOWLEDGEMENTS

The Authors extend their appreciation to the Deanship of Scientific Research at King Saud University for funding the work through the research group project NO. (RGP-VPP-041).

#### REFERENCES

- [1] Chattopadhyay, P., Chiu, Y.H., Lo, J.M., Chung, C.S. and Lu, T.H. (2000). Synthesis and structural characterization of a Re(V) complex with 2N1S donor and radiochemical behavior of its Tcanalog. *Applied Radiation and Isotopes*, **52**, 217-223. doi:10.1016/S0969-8043(99)00156-6
- [2] Papagiannopoulou, D., Pirmettis .I.C., Pelecanou, M., Tsoukalas, Ch., Raptopoulou, C.P., Terzis, A., Chiotellis, E and Papadopoulos, M. (2001) Synthesis and structural characterization of a novel Re[P][NN][S][SO] mixed ligand rhenium (III) complex. *Inorganica Chimica Acta*, **320**, 174-177.
- [3] Li . X-H., Tang, Z-X. and Zhang, X-Z. (2009) Molecular structure, IR spectra of 2-mercaptobenzothiazole and 2-mercaptobenzoxazole by density functional theory and ab initio Hartree-Fock calculations. *Spectrochimica Acta Part A: Molecular and Biomolecular Spectroscopy*, **74**, 168-173. doi:10.1016/j.saa.2009.05.026
- [4] Zhang H., Dai, M., Qi,C., Li. B. and Guo. X. (2004) Synthesis, biodistribution and quantitative structure-activity relationship studies of new  $^{99\text{m}}\text{Tc}$  labeled pseudo-peptide complexes. *Applied Radiation and Isotopes*, **60**, 643-651. doi:10.1016/j.apradiso.2003.08.010
- [5] Dhara, B., Chattopadhyay, P. (2005) New oxorhenium(V) complexes with 2N2S donor sets and radiochemical behavior of their technetium analogs. *Applied Radiation and Isotopes*, **62**, 729-735. doi:10.1016/j.apradiso.2004.10.002
- [6] Bouziotis, P., Pirmettis, I., Pelecanou, M., Raptopoulou, C.P., Terzis, A., Papadopoulos, M. and Chiotellis, E. (2001) Novel Oxorhenium and Oxotechnetium Complexes from an Aminothiols[NS]/Thiol[S] Mixed-Ligand System. *Chemistry—A European Journal*, **7**, 3671-3680. doi:10.1002/1521-3765(20010903)7:17<3671::AID-CHEM3671>3.0.CO;2-L
- [7] Gaussian 98 program, Gaussian, Inc. Pittsburgh, PPA 15106 USA.
- [8] Becke A.D and Pérez-Jordá, J. (1995) A density-functional study of van der Waals forces: rare gas diatomics. *Chemical Physics Letters*, **233**, 134-137. doi:10.1016/0009-2614(94)01402-H
- [9] Parr, R.G. and Liu .S. (2000) Homogeneities in density of various LDA energy functional. *Journal of Molecular Structure: Theochem*, **501-502**, 29-34. doi:10.1016/S0166-1280(99)00410-8
- [10] Hay, P.J., Chen, S.P., Voter, A.F., Albers, R.C., Boring, A.M. (1989) Theoretical studies of grain boundaries in Ni3Al with boron or sulfur. *Scripta Metall*, **23**, 217-222.
- [11] Glendening, E.D, Reed., A.E, Carpenter, .J.E and Weinhold, F, NBO (version 3.1).
- [12] Casida, M.E, (1996) Recent Development and Applications in Modern Density Functional Theory. In: Seminario, J.M. Ed., **4**, Elsevier, Amsterdam.
- [13] Machura ,B., Kruszynski, R. and Kusz, J. (2008) Novel oxorhenium complexes with 2-(20-hydroxyphenyl)-2-benzothiazolinato ligand: X-ray studies, spectroscopic characterization and DFT calculations. *Polyhedron*, **27**, 1679-1689. doi:10.1016/j.poly.2008.02.018
- [14] Machura, B., Kruszynski, R., Jaworska, M and Lodowski, P. (2005) Reactivity of  $[\text{ReOX}_3(\text{PPh}_3)_2]$  complexes towards 1,4-diaminobenzene: X-ray structure and DFT calculations. *Polyhedron*, **24**, 1454-1460. doi:10.1016/j.poly.2005.03.094
- [15] Giglio, J., Rey, A., Cerecetto, H., Pirmettis, I., Papadopoulos, M., León, E., Monge, A., López de Ceráin, A., Azqueta, A., González, M., Fernández, M., Paolino, A. and León, A (2006) Design and evaluation of “3 + 1”

- mixed ligand oxorhenium and oxotechnetium complexes bearing a nitroaromatic group with potential application in nuclear medicine oncology. *European Journal of Medicinal Chemistry*, **41**, 1144-1152. [doi:10.1016/j.ejmech.2006.05.006](https://doi.org/10.1016/j.ejmech.2006.05.006)
- [16] Machura, B., Kruszynski, R. and Kusz., J. (2007) *Polyhedron*, **26**, 1590-1596. [doi:10.1016/j.poly.2006.11.034](https://doi.org/10.1016/j.poly.2006.11.034)
- [17] Yatirajam .V. and Lakshmi Kantan .M. (2001) Synthesis and characterization of  $\text{ReOCl}_3(\text{DTO})_2$  and  $\text{ReOCl}_3(\text{MBT})_2$  complexes, *Polyhedron*, **2**, 1199-1200. [doi:10.1016/j.poly.2006.11.034](https://doi.org/10.1016/j.poly.2006.11.034)
- [18] References and further reading may be available for this article. To view references and further reading y
- [19] Pelecanou. M., Pirmettis. I.C., Nock. B.A., Papadopoulos. M., Chiotellis. E. and Stassinopoulou C.I. (1998) Interaction of  $[\text{ReO}(\text{SNS}) (\text{S})]$  and  $[\text{99mTcO}(\text{SNS}) (\text{S})]$  mixed ligand complexes with glutathione: Isolation and characterization of the product. *Inorganica Chimica Acta*, **281**, 148-152. [doi:10.1016/S0020-1693\(98\)00159-5](https://doi.org/10.1016/S0020-1693(98)00159-5)
- [20] Machura., B. (2005) Structural and spectroscopic properties of dinuclear rhenium complexes containing  $(\text{ReO})_2(\mu\text{-O})$  core. *Coordination Chemistry Reviews*, **249**, 591-612. [doi:10.1016/j.ccr.2004.07.007](https://doi.org/10.1016/j.ccr.2004.07.007)
- [21] Machura, B., Penczek, R., Kruszynski, (2007) Reactivity of  $[\text{ReOX}_3(\text{PPh}_3)_2]$  complexes towards pyridazine. X-ray structures of  $[\{\text{ReOC12}\}_2(\mu\text{-O})(\mu\text{-pyd})_2]\cdot\text{C}_6\text{H}_6$  and  $[\{\text{ReOBr}_2\}_2(\mu\text{-O})(\mu\text{-pyd})_2]\cdot\text{CH}_3\text{CN}$ , and DFT calculations for  $[\{\text{ReOC12}\}_2(\mu\text{-O})(\mu\text{-pyd})_2]$ . *Polyhedron*, **26**, 3054-3062. [doi:10.1016/j.poly.2007.02.019](https://doi.org/10.1016/j.poly.2007.02.019)
- [22] Braband, H., Miroslavov, A.E., Lumpov, A.A., Sidorenko, G.V., Levitskaya, E.M., Gorshkov, N.I, Suglobov, D.N., Alberto, R., Gurzhiy, V.V., Krivovichev, S.V and Tananaev, I.G. (2008) Complexes of technetium (I) ( $99\text{Tc}$ ,  $99\text{mTc}$ ) pentacarbonyl core with  $\pi$ -acceptor ligands (tert-butyl isocyanide and triphenylphosphine). *Journal of Organometallic Chemistry*, **693**, 4-10.